DOI: 10.1515/adms-2017-0008
M. Bartmanski

Gdansk University of Technology, Department of Materials Science and Welding Engineering, Narutowicza 11/12, 80-233 Gdańsk, Poland
michal.bartmanski@pg.gda.pl

THE PROPERTIES OF NANOSILVER – DOPED NANOHYDROXYAPATITE COATING ON THE Ti13Zr13Nb ALLOY

ABSTRACT

The aim of this research was to study the properties of nanohydroxyapatite (nanoHAp) and nanohydroxyapatite, doped with nanosilver (nanoHAp/nanoAg), coatings obtained by an electrophoretic deposition process. The suspensions was prepared by dispersing 0.1 g of HAp nanopowder for nanoHAp coatings and 0.1 g of nanoHAp and 0.025 g nanoAg for nanoHAp/nanoAg coatings. The deposition was carried out for 1 min at 50 V voltage followed by drying at room temperature for 24 h and heating at 800°C for 1 h in vacuum. The thickness of the nanoHAp and nanoHAp/nanoAg coatings was found as of about 5 μm. The corrosion behavior tests made by potentiodynamic methods brought out slightly higher values of corrosion current for nanoHAp coatings and nanoHAp/nanoAg coatings as compared to the reference Ti13Zr13Nb specimen. The nanohardness of the nanoHAp coatings achieved 0.020 ± 0.004 GPa and of the nanoHAp/nanoAg coatings 0.026 ± 0.012 GPa. Nanoscratch test of the nanoHAp and nanoHAp/nanoAg coatings revealed an increased Critical Friction (mN) in the presence of nanosilver particles. The wettability angles decreased for nanoHAp/nanoAg coatings comparing to pure nanoHAp coatings on titanium alloy.

Keywords*: nanohydroxyapatite coatings, nanosilver, titanium alloy, electrophoretic deposition*

INTRODUCTION

The titanium alloy (such as Ti6Al4V and less Ti6Al7Nb and Ti13Zr13Nb) nowadays are the most frequently used materials for load-bearing orthopedic implants because of their high biocompatibility and proper mechanical properties [1–6]. There are some reports on possible adverse e effects of both alloying elements of the Ti6Al4V: vanadium may provoke cytological responses and neurogenic disorders, and aluminum softens bone, do damage to nerve cells and disturbance of the function of enzymes [7–10]. The titanium alloy Ti13Zr13Nb possesses no harmful elements (aluminum and vanadium), is characterized by relatively low Young modulus (~ 80 GPa) [8] compared to Ti6Al4V (~110 GPa) [11] and is more mechanically compatible with the bone (15 - 20 GPa) [12,13].

To improve biocompatibility and mechanical properties, the different surface modification techniques were used like e.g. nanooxidation [8], laser treatment [14] or hydroxyapatite deposition [15]. Many deposition methods of hydroxyapatite/

nanohydroxyapatite were so far investigated, such as electrophoretic deposition (EPD) [16], plasma spraying [17], sol-gel methods [18] and biomimetic deposition [7]. In this research, the author obtained nanohydroxyapatite coatings on titanium alloy using electrophoretic deposition (EPD) method. EPD technique could be use to obtain thin films of hydroxyapatite. EPD process is a simple technique used for fabricated HAp and nanoHAp coatings. The main advantage of EPD is to produce porous coatings for enhancement of the bone growth into the porous structure of the coating. To prevent the shrinkage of ceramic nanohydroxyapatite coating after EPD, the sample should to sintered at the vacuum atmosphere at 800-1200º C [15]. The post-surgery treatment after implantation is carried out by an administration of antibiotics. To provide antibacterial properties of the hydroxyapatite coatings, the doping of nanosilver or nanocopper nanoparticles with similar bactericidal effects as antibiotics was investigated [6,19,20]. The bactericidal action of silver was proven for *Escherichia coli, Staphylococcus aureus, Staphylococcus albus, Candida albicans* and *Pseudomonas aeruginosa* [21–23]. To improve antibacterial properties of nanosilver, the sufficient content of nanosilver concentration around a tissue is needed. The minimum required value of silver concentration with bactericidal effect is 0.1 ppm, and value of cytotoxic concentration silver is 1.6 ppm [24]. The hydroxyapatite with Ag content less than 1 at. % demonstrated an excellent resistance to the bacteria attack [25].

The nanohydroxyapatite coatings doped silver were investigated in the past, but not for the Ti13Zr13Nb alloy. In present research, the deposition of nanohydroxyapatite coatings decorated with nanosilver on the Ti13Zr13Nb alloy was performed followed by examinations of microstructure, and chemical, corrosion, and mechanical properties of the coatings.

EXPERIMENTAL

Preparation of specimen

The specimens Ti13Zr13Nb of 4 mm in thickness and 15 mm in radius, cut from the rods, were prepared. The specimens were polished with abrasive paper, grid 2000# as the last. Then specimens were rinsed with isopropanol and ultrasonically cleaned (Sonic-3, POLSONIC, Poland) in distilled water for 15 min, pickled in 25% HNO_3 for 10 min to remove oxide layers from the substrate [26] and finally thoroughly rinsed with distilled water prior to deposition.

Electrophoretic deposition of nanoHAp and nanoHAp/nanoAg coatings

The electrophoretic deposition (EPD) was carried out in a suspension prepared by dispersing 0.1 g of HAp nanopowder with average particle size about 20 nm (MK Nano Canada) and 0.025 g of nanosilver with average particle size about 50 nm (Hongwu International Group LTD, China) in 100 mL of anhydrous ethanol. The suspensions were obtained by ultrasonic mixing for 60 min at room temperature. The Ti13Zr13Nb substrate was used as a cathode and platinum as a counter electrode. The electrodes were placed parallel to each other withina distance of 10 mm and connected to the DC power source (MCP/SPN110-01C, Shanghai MCP Corp., China). The electrophoretic deposition was performed at 50 V for 1 min at room temperature. Specimen were air dried at room temperature for 24 h. Finally, the coated Ti13Zr13Nb specimens were thermally treated in a tubular furnace (PROTHERM PC442, Ankara, Turkey) in a vacuum at 800°C for 120 min. They were heated from room temperature to 800°C at a rate 200°C/h and cooled to room temperature in the furnace.

Structure of nanoHAp and nanoHAp/nanoAg coatings

The coatings` surfaces and cross-sections were observed using a high resolution Scanning Electron Microscope (SEM JEOL JSM- 6480). The chemical composition of the coatings was investigated by the X-ray energy dispersive spectrometer (EDS), Edax Inc., U.S.A.

Corrosion behavior of nanoHAp and nanoHAp/nanoAg coatings in SBF

The electrochemical measurements of corrosion parameters were made for nanoHAp and nanoHAp/nanoAg coated Ti13Zr13Nb alloy by a potentiodynamic mode in simulated body fluid (SBF) at room temperature. The SBF was prepared according to PN-EN ISO 10993-15 [27] by dissolving reagent grade chemicals: $(NH_2)_2CO$ (0.13 gL^{-1}), NaCl (0.7 gL^{-1}), $NaHCO_3$ (1.5 gL^{-1}), Na_2HPO_4 (0.26 gL^{-1}), K_2HPO_4 (0.2 gL^{-1}), KSCN (0.33 gL^{-1}), KCl (1.2 gL^{-1}). A 3-electrode cell set-up was used with a standard platinum electrode as a counter and an Ag/AgCl (saturated with potassium chloride KCl) as a reference electrode. All experiments were performed using a potentiostat/galvanostat (Atlas 0531, Atlas Sollich, Poland). Before the experiment, the samples were stabilized at their open circuit potential (OCP) for 5 min. The potentiodynamic polarization test was made at a potential change rate of 1 mV/s, within a scan range from -600 mV to 2000 mV. From the polarization curves, the corrosion potential (E_{corr}) and corrosion current density (I_{corr}) were determined by the Tafel extrapolation method.

Mechanical studies – nanoindentation and nano scratch-test

Nanoindentation tests were performed with the NanoTest™ Vantage (Micro Materials) using a Berkovich three-sided pyramidal diamond. The nanoHAp and nanoAg coatings were tested, with 10 independent measurement tests for each sample. The maximum applied force was equal to 5 mN, the loading and unloading rate were set up at 20 s and the dwell period at full load was 10 s. The distances between the subsequent indents were set up at 50 μm. During the indent, the load-displacement curve was determined by the Oliver and Pharr method. From the load–penetration curves, surface hardness (H) and Young's modulus (E) were calculated using integrated software. To calculate Young's modulus (E), the Poisson's ratio 0.3 was assumed for HAp coating.

Nano-scratch tests were performed with the NanoTest™ Vantage (Micro Materials) using a Berkovich three-sided pyramidal diamond. The scratch tests were carried out by increasing load from 0 mN to 200 mN at a loading rate 1.3 mN/s at a distance 500 μm. The adhesion of the coating based on the change in frictional force during the test.

Contact angle studies

The water contact angle measurements were carried out for the nanoHAp and nanoHAp/nanoAg coatings by the contact angle instrument (Contact Angle Goniometer, Zeiss, Germany) at room temperature. All measurements were repeated three times for each specimen.

RESULTS AND DISCUSSION

Fig. 1 demonstrates the surfaces of nanoHAp and nanoHAp/nanoAg deposits, after thermal treatment obtained by electrophoretic deposition process at 50 V and 1 min from two different suspensions. The uniform sound quality of nanoHAp and nanoHAp/nanoAg coatings

appear. The color change of the nanoHAp/nanoAg coatings compared with pure nanoHAp coating suggests the presence of nanoparticles Ag inside the coating.

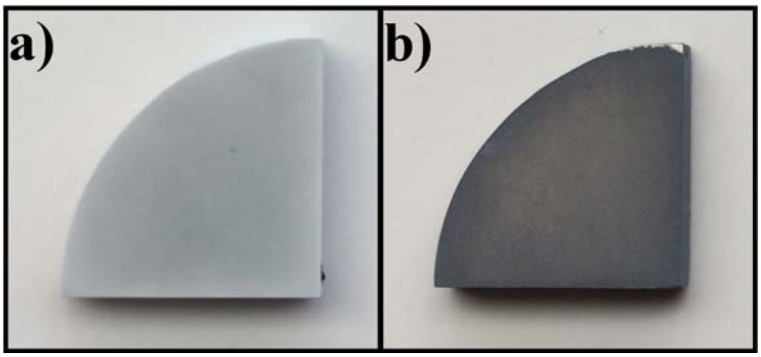

Fig. 1. NanoHAp (a) and nanoHAp/nanoAg (b) coatings obtained by EPD process at 50 V / 1 min, after thermal treatment

Fig. 2. shows the SEM images of nanoHAp and nanoHAp/nanoAg coatings and EDS spectra for both coatings. The cracks and agglomerations appear on both types of coatings, in particular on the nanoHAp coating, for which a greater number of longer cracks is seen.

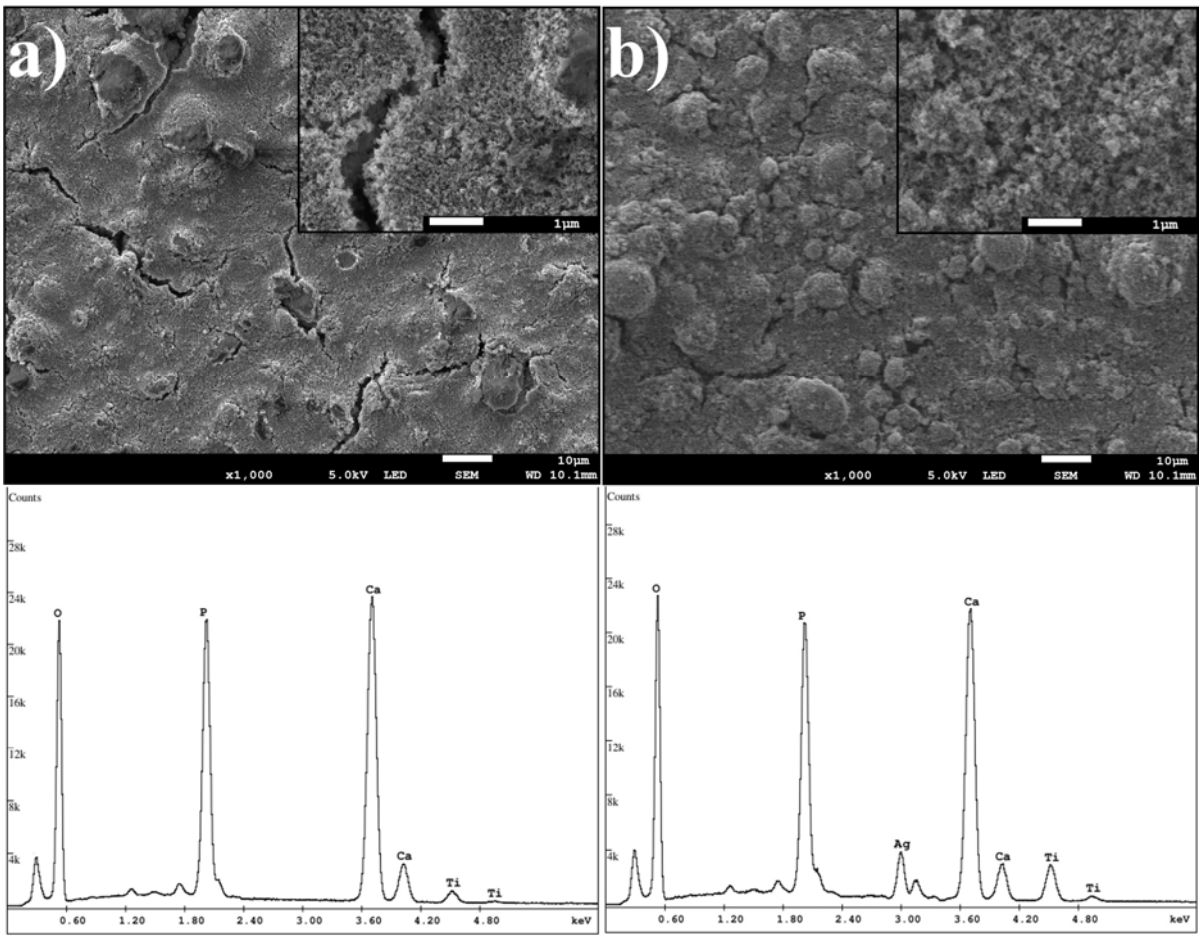

Fig. 2. SEM images (with different magnifications) and EDS spectra of the nanoHAp (a) and nanoHAp/nanoAg (b) coatings after thermal treatment

The agglomeration of nanoHAp particles is due to faster kinetics of the migration process and low time to find and occupy the most suitable positions to form a uniform coating [28,29]. NanoHAp/nanoAg coating compared with the nanoHAp coating are characterized by a smaller number of cracks what may be due to the presence of silver nanoparticles inside the coating and reducing the internal stress inside the coating after the thermal treatment. EDS spectra reveal the presence of the same elements in both coatings – oxygen (O), potassium (P), calcium (Ca) and titanium (Ti). O, P and Ca elements indicate the presence of hydroxyapatite, the presence of Ti element results from the small thickness of the coatings.

Fig. 3. illustrates the thickness of the coatings. The thickness of the nanoHAp coatings was 5.16 ± 0.53 μm and of nanoHAp/nanoAg was 4.97 ± 1.15 μm. The large standard deviation
originates from the large surface roughness characteristic for hydroxyapatite coatings. The effect of nanosilver presence is negligible – nanosilver particles probably did not significantly affect the particles` migration during the electrophoretic deposition process. The cross-sections also illustrate that both nanoHAp coatings are well adjacent to the Ti13Zr13Nb substrate without any delamination.

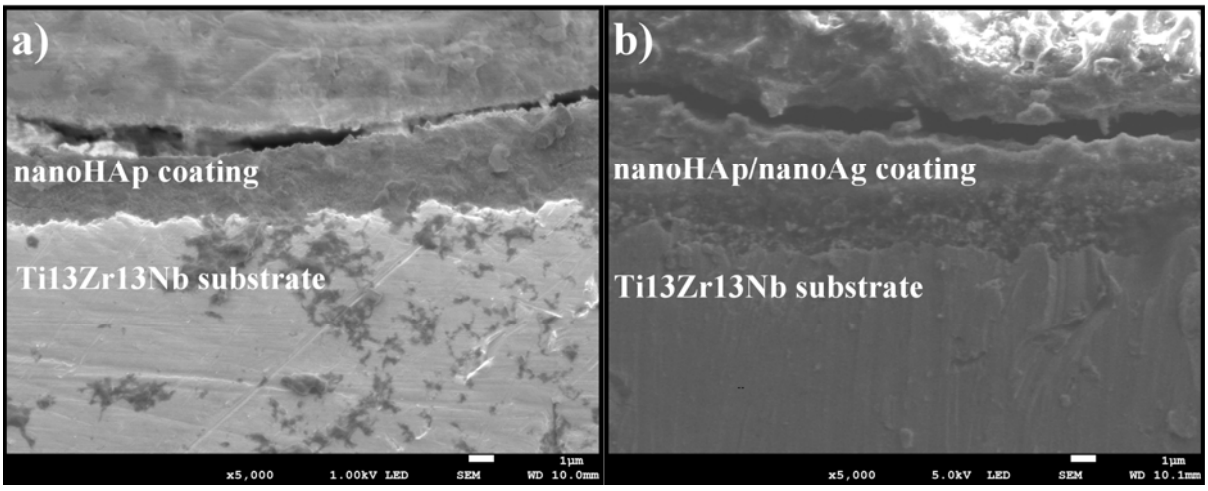

Fig. 3. Cross-sections of (a) nanoHAp and (b) nanoHAp/nanoAg coatings after thermal treatment

Fig. 4 and Tab. 1 show the effect of nanoHAp and nanoHAp/nanoAg coatings on corrosion current compared with undercoated Ti13Zr13Nb reference specimen.

The results prove that undecorated reference alloy is characterized by the greatest corrosion resistance compared with nanoHAp and nanoHAp/nanoAg coatings. This may be the resultof localized corrosion occurring due to the small thickness and porous structure of both types of the coatings. The presence of nanosilver particles increases the corrosion current density again. On the other hand, the corrosion rate is still at a minimal level. The investigationsof nanoHAp/nanoAg coatings were already performed, but for thick coatings or coatingson TiO_2 layers [24,30].

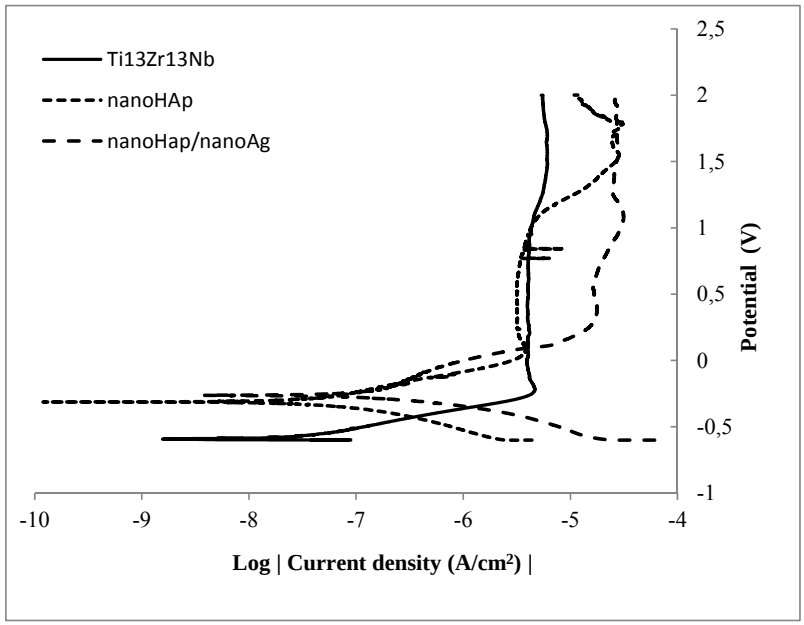

Fig. 4. Potentiodynamic polarization curves of nanoHAp, nanoHAp/nanoAg coating and reference specimen Ti13Zr13Nb in SBF at room temperature

Table 1. *Corrosion current density and corrosion potential of nanoHAp, nanoHAp/nanoAg coatings and uncoated Ti13Zr13Nb substrate*

Sample	E_{cor} [mV]	i_{cor} [nA/cm^2]
reference Ti13Zr13Nb alloy	- 487.26	51.92
nanoHAp coating	- 303.18	105.49
nanoHAp/nanoAg coating	- 252.32	219.13

Fig. 5 and Tab. 2 show the effect of nanosilver presence on nanomechanical properties of the coatings. Fig. 5 show the typical curves for nanoHAp and nanoHAp/nanoAg coatings obtained during the nanoindentation tests. The curves for nanoHAp and nanoHAp/nanoAg coating are similar.

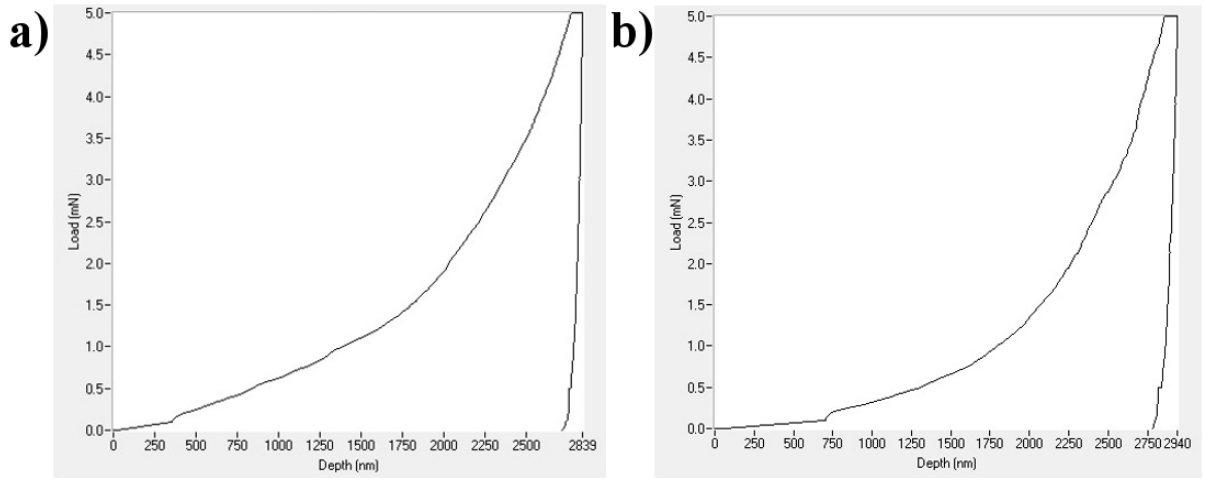

Fig. 5. Nanoindentation load-displacement curves carried out on the (a) nanoHAp and (b) nanoHAp/nanoAg coatings after thermal treatment

The mechanical properties of both types of coating differ slightly. The nanoHAp/nanoAg coating is characterized by a higher value of hardness. The values of Young's modulus are similar to each other. With increasing hardness, the decreasing maximum depth and plastic work are observed. The value of elastic work seems negligible for nanoHAp and nanoHAp/nanoAg coatings. The Young`s modulus is a crucial parameter, as it ensures a strong connection between the implant and the bone [3]. The materials to bone regeneration should have a value of Young`s modulus similar or lower that of a natural human bone (15 - 20 GPa) [12,13]. Poor mechanical properties caused the fast dissolution of the coatings in a physiological environment [31].

Table 2. *Mechanical properties and Nanoindentation properties of nanoHAp and nanoHAp/nanoAg coatings after thermal treatment*

Sample	Hardness [GPa]	Young's modulus (GPa)	Maximum depth (nm)	Plastic work (nj)	Elastic work (nj)
nanoHAp coating	0.020±0.004	5.39±0.89	3114.65±339.18	4.79±0.72	0.17±0.02
nanoHAp/nanoAg coating	0.026±0.012	5.57±1.69	2930.51±512.41	3.37±0.65	0.19±0.02

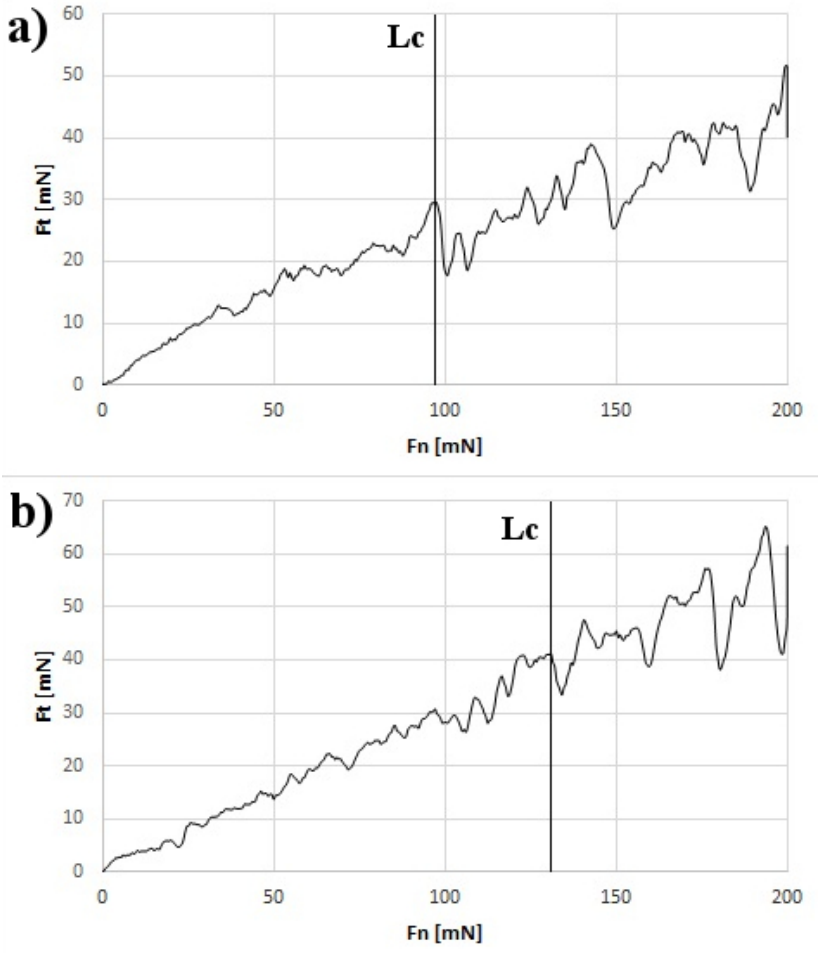

Fig. 6. Nanoscratch test the nanoHAp and nanoHAp/nanoAg coatings, after thermal treatment

The nano-scratch tests results for nanoHAp and nanoHAp/nanoAg coatings are shown in Fig. 6 and Tab. 3. Fig. 6 show the typical curves for nanoHAp and nanoHAp/nanoAg coatings obtained during the nano-scratch test. The *Lc* is the value of the Critical Load. The beginning of coatings' delamination can be determined based on s sudden change in friction force and normal force.

As can be seen, the presence of nanosilver particles has a significant impact on the value of Critical Friction and Critical Load. With the increased value of Critical Friction, the increased value of Critical Load appears as well. The lower value of hardness and Young's modulus indicates better adhesion of the nanoHAp coating deposited on the Ti13Zr13Nb substrate. The nanohydroxyapatite coatings obtained by Drevet et all using EPD technique have higher adhesion to the substrate, but the author does not provide the coating thickness, so it is impossible to compare the results [3] The excellent mechanical properties (as a coating adhesion to the substrate) are necessary for hydroxyapatite coatings for orthopedic implants because of high mechanical stress occurring during the implantation surgery [3].

Table 3. *Critical friction and Critical Load of the nanoHAp and nanoHAp/nanoAg coatings*

Sample	Critical Friction [mN]	Critical Load [mN]
nanoHAp coating	30.66±3.92	108.58±16.24
nanoHAp/nanoAg coating	40.58±4.94	123.99±22.10

Fig. 7 shows the effect of nanosilver particle presence on the water contact angle. The contact angle decreases significantly for nanoHAp/nanoAg coatings compared with nanoHAp coatings. The both types of coating have hydrophilic character what may be attributed to their porous surface structure. However nanoHAp/nanoAg coatings exhibits a lower contact angle (9.0 ± 0.1º) than nanoHAp coatings (40.6 ± 0.5º). The hydrophilic nature of the nanohydroxyapatite coatings is necessary to promote a cell attachment [32]. According to Heise et all. [33] the best values of contact angles for cell attachment were assessed at 55º and for bone regeneration at 35º to 80º, more than here.

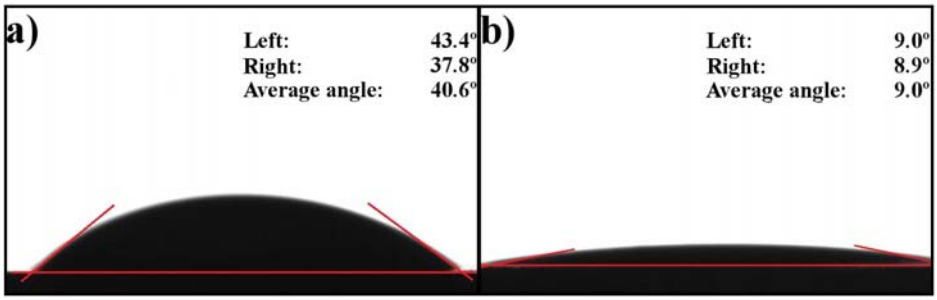

Fig. 7. Contact angle for water droplet on (a) nanoHAp and (b) nanoHAp/nanoAg coating

CONCLUSIONS

The electrophoretic deposition process (EPD) is the method which allows for obtaining homogeneous, thin, high corrosion resistant and of proper mechanical properties, hydrophilic nanoHAp or nanoHAp/nanoAg coatings on the Ti13Zr13Nb alloy.

The presence of nanosilver particles has a significant effect on homogeneity and quality of coating. On the coating with silver nanoparticiples smaller number of cracks and smaller dimension of cracks were observed. Unfortunately presents of nanosilver in coating reduced corrosion resistance. To provide better corrosion resistant in future it is possibility to deposition nanoHAp or nanoHAp/nanoAg coatings on $Ti0_2$ layer which possesses excellent corrosion-resistant properties. The presence of nanosilver particles in the coating improved adhesive properties and reduce of contact angle values. The influence of the presence of silver nanoparticles is negligible for the thickness of coatings and mechanical properties.

The nanohydroxyapatite nanoHAp or nanoHAp/nanoAg coatings obtained by electrophoretic deposition at 50 V for 1 min possess the sufficient mechanical and chemical propertiesto be used as biocompatible, bioactive and antibacterial coatings.

ACKNOWLEDGMENTS

The author thanks the employees of the Departments of Materials Engineering and Bonding for their help in preparation of SEM images and EDS spectra. The contribution in the development of the paper from Prof. Andrzej Zielinski is gratefully acknowledged.

REFERENCES

1. Zielinski A., Sobieszczyk S., Seramak T., Serbinski W., Swieczko-Zurek B., Ossowska A., Biocompatibility and Bioactivity of Load-Bearing Metallic Implants, Advances in Materials Sciences. 10 (2011) 21–31.
2. Bartmanski M., Berk A., Wojcik A., The Determinants of Morphology and Properties of the Nanohydroxyapatite Coating Deposited on the Ti13Zr13Nb Alloy by Electrophoretic Technique, Advances in Materials Science. 16 (2016) 56–66.
3. Drevet R., Ben Jaber N., Fauré J., Tara A., Ben Cheikh Larbi A., Benhayoune H., Electrophoretic deposition (EPD) of nano-hydroxyapatite coatings with improved mechanical properties on prosthetic Ti6Al4V substrates, Surface and Coatings Technology. 301 (2015) 94–99.
4. Kwok C.T., Wong P.K., Cheng F.T., Man H.C., Characterization and corrosion behavior of hydroxyapatite coatings on Ti6Al4V fabricated by electrophoretic deposition, Applied Surface Science. 255 (2009) 6736–6744.
5. Strakowska P., Beutner R., Gnyba M., Zielinski A., Scharnweber D., Electrochemically assisted deposition of hydroxyapatite on Ti6Al4V substrates covered by CVD diamond films - Coating characterization and first cell biological results, Materials Science and Engineering C. 59 (2016) 624–635.
6. Huang Y., Hao M., Nian X., Qiao H., Zhang H., Zhang X., Song G., Guo J., Pang X., Zhang H., Strontium and copper co-substituted hydroxyapatite-based coatings with improved antibacterial activity and cytocompatibility fabricated by electrodeposition, Ceramics International. 42 (2016) 11876–11888.
7. Pylypchuk I.V., Petranovskaya A.L., Gorbyk P.P., Korduban A.M., Markovsky P.E., Ivasishin O.M., Biomimetic Hydroxyapatite Growth on Functionalized Surfaces of Ti-6Al-4V and Ti-Zr-Nb Alloys, Nanoscale Research Letters. 10 (2015) 1–8.
8. Ossowska A., Sobieszczyk S., Supernak M., Zielinski A., Morphology and properties of nanotubular oxide layer on the "Ti-13Zr-13Nb" alloy, Surface and Coatings Technology. 258 (2014) 1239–1248.

9. Delgado-Alvarado C., Sundaram P.A., Corrosion evaluation of Ti-48Al-2Cr-2Nb (at.%) in Ringer's solution, Acta Biomaterialia. 2 (2006) 701–708.
10. Narayanan R., Seshadri S.K., Synthesis and corrosion of functionally gradient TiO2 and hydroxyapatite coatings on Ti-6Al-4V, Materials Chemistry and Physics. 106 (2007) 406–411.
11. Araghi A., Hadianfard M.J., Fabrication and characterization of functionally graded hydroxyapatite/TiO2 multilayer coating on Ti-6Al-4V titanium alloy for biomedical applications, Ceramics International. 41 (2015) 12668–12679.
12. Geetha M., Singh A.K., Asokamani R., Gogia A.K., Ti based biomaterials, the ultimate choice for orthopaedic implants - A review, Progress in Materials Science. 54 (2009) 397–425.
13. Manoj Kumar R., Kuntal K.K., Singh S., Gupta P., Bhushan B., Gopinath P., Lahiri D., Electrophoretic deposition of hydroxyapatite coating on Mg-3Zn alloy for orthopaedic application, Surface and Coatings Technology. 287 (2016) 82–92.
14. Majkowska B., Jazdzewska M., Wolowiec E., Piekoszewski W., Klimek L., Zielinski A., The Possibility Of Use Of Laser-Modified Ti6Al4V Alloy In Friction Pairs In Endoprostheses, Archives of Metallurgy and Materials. 60 (2015) 6–9.
15. Dudek K., Goryczka T., Electrophoretic deposition and characterization of thin hydroxyapatite coatings formed on the surface of NiTi shape memory alloy, Ceramics International. 42 (2016) 19124–19132.
16. Boccaccini R., Keim S., Ma R., Li Y., Zhitomirsky I., Electrophoretic deposition of biomaterials., Journal of the Royal Society, Interface / the Royal Society. 7 (2010) 581–613.
17. Xue W., Tao S., Liu X., Zheng Z., Ding C., In vivo evaluation of plasma sprayed hydroxyapatite coatings having different crystallinity, Biomaterials. 25 (2004) 415–421.
18. Asri R.I.M., Harun W.S.W., Hassan M.A., Ghani S.A.C., Buyong Z., A review of hydroxyapatite-based coating techniques: Sol-gel and electrochemical depositions on biocompatible metals, Journal of the Mechanical Behavior of Biomedical Materials. 57 (2016) 95–108.
19. Kobayashi Y., Shirochi T., Yasuda Y., Morita T., Synthesis of silver/copper nanoparticles and their metal-metal bonding property, Journal of Mining and Metallurgy, Section B: Metallurgy. 49 (2013) 65–70.
20. Chen Y., Zheng X., Xie Y., Ji H., Ding C., Li H., Dai K., Silver release from silver-containing hydroxyapatite coatings, Surface and Coatings Technology. 205 (2010) 1892–1896.
21. Zhang W., Chu P.K., Enhancement of antibacterial properties and biocompatibility of polyethylene by silver and copper plasma immersion ion implantation, Surface and Coatings Technology. 203 (2008) 909–912.
22. Stanić V., Janaćković D., Dimitrijević S., Tanasković S.B., Mitrić M., Pavlović M.S., Krstić A., Jovanović D., Raičević S., Synthesis of antimicrobial monophase silver-doped hydroxyapatite nanopowders for bone tissue engineering, Applied Surface Science. 257 (2011) 4510–4518.
23. Mohan S., Oluwafemi O.S., Songca S.P, Jayachandran V.P., Rouxel D., Joubert O., Kalarikkal N., Thomas S., Synthesis, antibacterial, cytotoxicity and sensing properties of starch-capped silver nanoparticles, Journal of Molecular Liquids. 213 (2016) 75–81.
24. Mirzaee M., Vaezi M., Palizdar Y., Synthesis and characterization of silver doped hydroxyapatite nanocomposite coatings and evaluation of their antibacterial and corrosion resistance properties in simulated body fluid, Materials Science and Engineering C. 69 (2016) 675–684.
25. Huang Y., Zhang X., Zhang H., Qiao H., Zhang X., Jia T., Han S., Gao Y., Xiao H., Yang H., Fabrication of silver- and strontium-doped hydroxyapatite/TiO2 nanotube bilayer coatings for enhancing bactericidal effect and osteoinductivity, Ceramics International. 43 (2017) 992–1007.

26. Mohan L., Durgalakshmi D., Geetha M., Sankara Narayanan T.S.N., Asokamani R., Electrophoretic deposition of nanocomposite (HAp + TiO 2) on titanium alloy for biomedical applications, Ceramics International. 38 (2012) 3435–3443.

27. Loch J., Krawiec H., Corrosion behaviour of cobalt alloys in artifical salvia solution, Archives of Foundry Engineering. 13 (2013) 101–106.

28. Farrokhi-Rad M., Shahrabi T., Effect of suspension medium on the electrophoretic deposition of hydroxyapatite nanoparticles and properties of obtained coatings, Ceramics International. 40 (2014) 3031–3039.

29. Abdeltawab A.A., Shoeib M.A., Mohamed S.G., Electrophoretic deposition of hydroxyapatite coatings on titanium from dimethylformamide suspensions, Surface and Coatings Technology. 206 (2011) 43–50.

30. Yan Y., Zhang X., Huang Y., Ding Q., Pang X., Antibacterial and bioactivity of silver substituted hydroxyapatite/TiO2 nanotube composite coatings on titanium, Applied Surface Science. 314 (2014) 348–357.

31. Clèries L., Fernández-Pradas J., Morenza J., Behavior in simulated body fluid of calcium phosphate coatings obtained by laser ablation, Biomaterials. 21 (2000) 1861–1865.

32. Huang Y., Hao M., Nian X., Qiao H., Zhang X., Zhang X., Song G., Guo J., Pang X., Zhang H., Strontium and copper co-substituted hydroxyapatite-based coatings with improved antibacterial activity and cytocompatibility fabricated by electrodeposition, Ceramics International. 42 (2016) 11876–11888.

33. Heise S., Höhlinger M., Torres Y., José J., Palacio P., Antonio J., Ortiz R., Wagener V., Virtanen S., Boccaccini A.R., Electrochimica Acta Electrophoretic deposition and characterization of chitosan / bioactive glass composite coatings on Mg alloy substrates, Electrochimica Acta. 232 (2017) 456–464.